A&A 460, 539–545 (2006)
DOI: 10.1051/0004-6361:20064828

Astronomy & Astrophysics

Near-infrared variability of a sample of galactic carbon Miras⋆,⋆⋆

F. Kerschbaum[1], M. A. T. Groenewegen[2], and C. Lazaro[3,4]

[1] Institute for Astronomy, University of Vienna, Türkenschanzstrasse 17, 1180 Vienna, Austria
e-mail: franz.kerschbaum@univie.ac.at
[2] Instituut voor Sterrenkunde, KU Leuven, Celestijnenlaan 200B, 3001 Heverlee, Belgium
[3] Dpto. de Astrofísica, Fac. de Física, Universidad de La Laguna, 38200 La Laguna, Tenerife, Spain
[4] Instituto de Astrofísica de Canarias, 38200-La Laguna, Tenerife, Spain

Received 9 January 2006 / Accepted 16 July 2006

ABSTRACT

Aims. In this paper we aim to determine the longest pulsation period of infrared carbon stars.
Methods. Forty-seven infrared carbon stars were selected based on (1) IRAS colours and spectral classification from the IRAS LRS atlas, and (2) known carbon stars with large CO expansion velocities. Multi-epoch *JHKL′* photometry was obtained.
Results. Reliable periods could be derived for 31 stars. The two longest periods are 840 and 870 days, only slightly longer than the previously longest known period for a galactic carbon star of 783 days. This is considerably shorter than the periods of some OH/IR stars. As the present survey targeted carbon stars that are likely to be among those with the longest periods expected, this difference appears real. To try to understand the longest observed period, the synthetic AGB code of Wagenhuber & Groenewegen (1998, A&A, 340, 183) was fine-tuned to reproduce the models of Vassiliadis & Wood (1993, ApJ, 413, 641). For several initial masses the fundamental mode period distribution was calculated for stars inside observed instability strip. Depending on details of the adopted mass loss rate, it is found that the mass limit where a carbon star has a probability of less than 1% of being in the observed instability strip with a period longer than 900 days is between 2.6 and 3.1 $M_{\odot}$.
Conclusions. Synthetic AGB calculations suggest that the observed upper limit in period can be interpreted as an upper mass limit of carbon star formation, with a value of between 2.6 and 3.1 $M_{\odot}$, depending on the adopted AGB mass loss rate. Such a mass limit is predicted by stellar evolution through the occurence of Hot Bottom Burning where (dredged-up) carbon is converted into nitrogen; this is predicted to occur at higher masses (∼4 $M_{\odot}$), although this depends on convection and core overshoot.

Key words. stars: carbon – stars: AGB and post-AGB – stars: variables: general – infrared: stars

1. Introduction

Pulsation is a critical aspect of the late stages of stellar evolution. The longest known indication of these pulsations are the well-expressed regular and irregular variations in brightness of objects on the Asymptotic Giant Branch (AGB) like Mira-, Semiregular (SRV), and Irregular Variables (IRV). This pulsation affects the structure of the stellar atmosphere. As it drives the extension of the outer stellar layers, it produces an environment for the formation of dust, which is an important factor for the mass loss and therefore for the stellar evolution.

The theoretical description of the pulsational phenomena in the atmosphere of AGB stars is now making considerable progress (e.g., Höfner et al. 1998; Höfner 1999; Winters et al. 2000; Nowotny et al. 2005, and references therein).

Moreover, for the more regular pulsators among the AGB variables, well established Mira period-luminosity and period-K magnitude relations are available (e.g., Feast et al. 1989; Groenewegen & Whitelock 1996), allowing for a reliable determination of distances to individual field stars or even outside the local group (e.g., the Miras in Cen A, Rejkuba 2004).

The results from the micro-lensing surveys are very impressive (e.g., Wood et al. 1999; Ita et al. 2004; Groenewegen 2004; Fraser et al. 2005) and have revealed several sequences that can be interpreted as being due to the fundamental mode pulsation of the Mira variables, and overtone pulsation for the smaller amplitude variables.

Also, robotic large area or even all sky surveys like the All Sky Automated Survey (ASAS, Pojmanski 2002) or the Northern Sky Variability Survey (NSVS, Wozniak et al. 2004) provide valuable and systematic information on AGB variability (see also Sect. 3.1).

Nevertheless, these surveys have been carried out in the optical and therefore miss the most obscured stars that undergo significant mass loss and then become faint to invisible in the optical. One should note that Kiss & Bedding (2004) and Groenewegen (2004) did find a large number of very red ($J - K \gg 1.4$ mag) "faint Miras" in the OGLE-II observations of the SMC, which fall below the fiducial Mira P-L relation by 1.5–2 mag in K and 4–6 mag in I, so that they are very likely candidates for being obscured carbon-rich Mira stars.

The pulsational properties of such stars are poorly studied, in particular the carbon-rich ones, the so-called "infrared carbon stars". Few periods have been determined, except, e.g., by Jones et al. (1990) and Le Bertre (1992). Interestingly, the longest known period for a carbon star is around 780 days in the Galaxy (AFGL 809, AFGL 2494, Jones et al. 1990) and near 940 days in the LMC (IRAS 05190–6748, Whitelock et al. 2003), while

⋆ Based on observations made with the Carlos Sánchez Telescope operated on the island of Tenerife by the Instituto de Astrofísica de Canarias (IAC) in the Observatorio del Teide, Izaña.
⋆⋆ Appendix A is only available in electronic form at http://www.aanda.org

among the dust obscured oxygen-rich stars (often called OH/IR stars), periods of well over a 1000 days and up to 2800 days are known (e.g., van Langevelde et al. 1990). Is this an evolutionary effect?

From observations in the LMC and SMC, it has become clear that the brightest AGB stars are not carbon stars, but MS and S-stars (e.g., Smith et al. 1995). This should be reflected in the periods carbon stars can attain. It is clear however that many more periods for infrared carbon stars are needed to quantify this.

Therefore, we present in this paper new multi-epoch near-infrared photometry of a sample of IR bright, high mass loss carbon stars not studied in the optical range at all. For most of the objects in our sample this is the first measurement of their infrared light change.

2. The sample and observations

The sample was selected as follows: as a first step stars with an IRAS LRS classification of 4n, suggestive of a carbon star as it indicates the presence of the silicon carbide dust feature (this was verified visually), and IRAS fluxes $S25 > 0.4 \times S12$ and $S12 > 50$ Jy were selected from the IRAS PSC. The former criterium selects carbon stars that, based on existing data, preferentially contain stars with $P > 500$ days. The latter criterium ensures that even the reddest stars can be observed in K and L ($K < 10$), while the bluer stars can be monitored in *JHKL*. In addition, carbon stars with expansion velocities larger than about 23 km s^{-1} (selected from the catalogue of CO measurements of Loup et al. 1993) were added to the sample with the rationale that high expansion velocities are a sign of high luminosities in the theory of radiation driven wind (Elitzur & Ivezić 2001) and carbon stars with high luminosities based on reasonably well determined kinematic distances (Kastner et al. 1993). Those additional stars that are outside the colour and/or flux criterium were only included if existing NIR data indicated that they are not too faint.

The observations were carried out at the Observatorio del Teide, the 1.5 m "Carlos Sánchez Telescope" of the Instituto de Astrofísica de Canarias (IAC) on Izaña, Tenerife was used with the "CVF Photometer-Spectrophotometer". The L-filter there is actually L' (3.78 μm).

All sources were searched for at their IRAS positions, mostly in filter K. A diaphragm of 15″ was used; beam-switching was done in the East-West direction with a throw of generally 20″. Standard and programme stars were observed at similar air mass ranges to avoid the nonlinear effects of atmospheric extinction in the infrared. The *JHKL'*-photometry was calibrated on the Koornneef (1983a,b) system.

The observations were done by the authors during 25 dedicated runs between September 1995 and August 1999. A few additional measurements where carried out by Stefano Bagnulo and Mathias Schultheis.

3. Results

3.1. Period finding

As noted already in Lebzelter (1999), classical methods for deriving a period, like Fourier analysis (Sperl 1998), alone do not always provide satisfying results for light curves of AGB variables. We therefore combined it with visual inspection (maxima, minima) and least square fitting techniques (Sperl 1998).

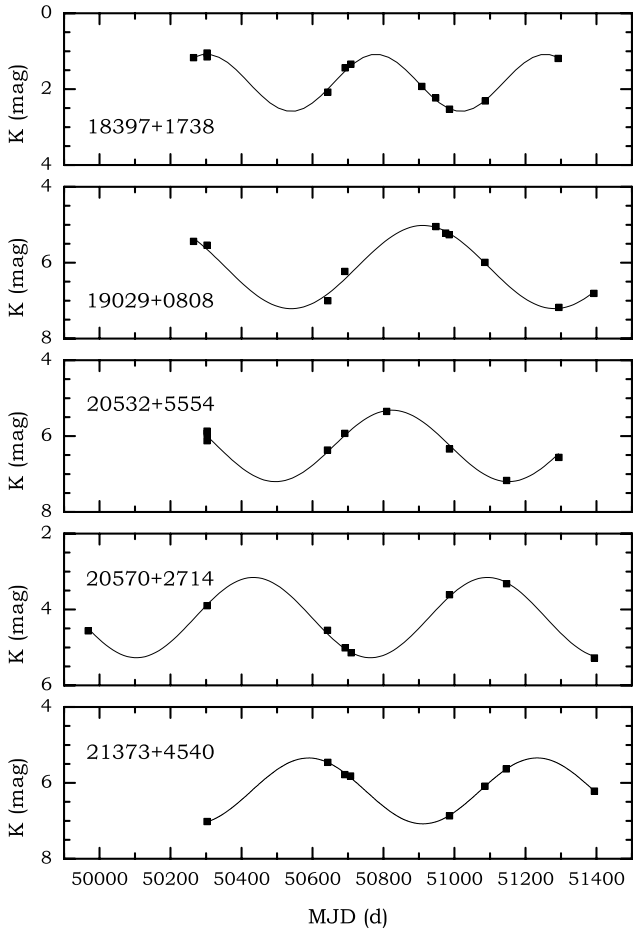

Fig. 1. Examples of K-band photometry for 5 stars with corresponding fit solutions.

To illustrate the typical K-band variability of these stars we plotted the K-band light curves of five stars from our sample in Fig. 1. To allow a direct comparison of amplitude and period of the variation we used the same scaling for all stars shown.

The formal frequency uncertainty Δf from Fourier analysis is indirectly proportional to the sample length ΔT. A practical rule of thumb $\Delta f = 1.5/\Delta T$ comes from Loumos & Deeming (1978), which corresponds, for our data sets (ΔT typically 1000 days, which is of the same order as the expected periods) in the period domain, to ΔP of about 135, 375, and 735 days for periods of 300, 500, and 700 days, respectively. These very conservative values are considerably improved to about 10% of the period, when least-square fitting techniques are carried out, but one should keep in mind this principal limitation, which can only be overcome by a longer time base. Another limitation is the density of the sampling, which is responsible for the high frequency, i.e. short period cut-off. For our sampling (say 10 points in 1000 days, a typical Nyquist cut-off is found at around 200 days in period, below the expected periods of long period variables. A detection of more rapid variations or the detailed shape of the light curves would require a much better sampling.

Table 1 gives an overview of the resulting periods derived from the K-band light curves as well as the correponding amplitudes (used in the mathematical sense, i.e., half of the peak-to-peak variation). Moreover, mean colours of the fitted light curves are calculated. Only in the two cases where no period solutions could be found were straight average colours calculated. n gives

Table 1. Mean near-infrared photometry, variability, luminosity and distance. *n* gives the number of datapoints in the corresponding filter. A ":" after the *K*-band amplitude indicates uncertainties in period and amplitude determination. Luminosity and distance information is derived via the *PL* relation discussed in the text.

IRAS	Variable	Name	J_m	H_m	K_m	L'_m	n_J	n_H	n_K	$n_{L'}$	P_K (d)	A_K		M_K	M_{bol}	L ($L_\odot$)	r_K (pc)
01105+6241	NSV 438	AFGL177	5.27	3.63	2.35	0.56	7	7	7	4	711	1.32	:	−9.01	−5.37	1.08×10^4	1.87×10^3
02152+2822	YY Tri		12.75	10.13	7.05	2.62	5	7	7	2	841	0.77		−9.27	−5.55	1.29×10^4	1.84×10^4
03192+5642	KX Cam		9.14	6.91	5.20	3.44	8	8	8	3	795	0.98	:	−9.19	−5.49	1.22×10^4	7.54×10^3
03238+6034	KY Cam	AFGL4277	11.42	8.51	6.10	2.93	7	10	10	4	642	0.86		−8.86	−5.25	9.75×10^3	9.81×10^3
03385+5927			12.32	9.61	6.92	3.42	6	10	10	2	629	1.02		−8.82	−5.23	9.54×10^3	1.41×10^4
03448+4432		AFGL5102	13.69	10.47	7.24	2.99	6	8	8	3	729	0.73		−9.05	−5.39	1.11×10^4	1.81×10^4
04179+5951		AFGL5118	10.76	8.03	5.76	2.90	3	7	7	1	536	0.88	:	−8.58	−5.05	8.08×10^3	7.36×10^3
05136+4712			11.65	9.14	6.85	3.46	6	9	9	4	552	0.85		−8.62	−5.08	8.33×10^3	1.24×10^4
06088+1909			8.42	6.25	4.44	2.12	7	7	7	1	405	0.68		−8.14	−4.73	6.04×10^3	3.28×10^3
06226−0905	V636 Mon	AFGL933	4.96	3.32	1.99	0.50	5	5	5	3	490	0.78	:	−8.44	−4.95	7.37×10^3	1.22×10^3
06268+0849	V477 Mon	AFGL5196	8.34	6.25	4.32	1.72	6	6	6	3	422	0.74	:	−8.21	−4.78	6.31×10^3	3.19×10^3
06487+0551			8.82	6.48	4.53	2.03	6	6	6	2	552	0.55	:	−8.62	−5.08	8.33×10^3	4.26×10^3
06531−0216		AFGL1039	6.93	5.12	3.62	1.83	6	6	6	1	*no solution*						
17581−1744		AFGL2047	8.07	5.89	4.12	1.82	10	10	10	5	590	0.71		−8.72	−5.16	8.93×10^3	3.71×10^3
18040−0941	FX Ser	AFGL2067	6.56	4.21	2.45	0.35	8	8	8	4	605	0.67		−8.76	−5.19	9.17×10^3	1.75×10^3
18239−0655	NSV 24440	AFGL2154	10.11	7.38	4.79	1.34	8	9	9	3	638	0.72	:	−8.84	−5.24	9.68×10^3	5.34×10^3
18240+2326	V1076 Her	AFGL2155	11.76	9.29	6.02	1.42	7	8	8	5	662	0.93		−8.90	−5.29	1.01×10^4	9.67×10^3
18244−0815			11.16	8.49	5.83	2.72	5	7	7	5	695	0.61		−8.98	−5.34	1.06×10^4	9.13×10^3
18248−0839			12.66	9.42	6.34	2.25	6	6	8	4	652	1.01		−8.88	−5.27	9.89×10^3	1.10×10^4
18269−1257			13.70	10.35	7.35	3.56	2	5	6	1	872	1.97		−9.33	−5.60	1.34×10^4	2.16×10^4
18320−0352		AFGL7012	13.11	11.13	8.20	3.94	3	4	6	3	596	0.77	:	−8.74	−5.17	9.01×10^3	2.45×10^4
18367−0452			12.22	10.62	8.02	3.62	6	7	8	4	649	0.95		−8.87	−5.26	9.85×10^3	2.39×10^4
18397+1738	V821 Her	AFGL2232	5.56	3.60	1.83	–0.74	11	11	11	7	478	0.75		−8.40	−4.92	7.17×10^3	1.11×10^3
18398−0220	V1417 Aql	AFGL2233	5.47	3.40	1.71	–0.50	7	7	7	2	687	0.56		−8.96	−5.33	1.04×10^4	1.36×10^3
18424+0346			9.42	6.95	4.91	2.26	8	8	8	2	456	1.07		−8.33	−4.87	6.83×10^3	4.43×10^3
18475+0926		AFGL2259	11.58	9.20	6.41	2.22	8	10	10	4	610	0.80		−8.78	−5.19	9.24×10^3	1.09×10^4
19029+0808	NSV 24681	AFGL2316	11.45	9.08	6.11	2.05	7	10	10	4	742	1.10		−9.08	−5.41	1.13×10^4	1.09×10^4
19029+2017		AFGL2318	7.83	5.65	3.86	1.84	6	6	6	3	594	0.68		−8.73	−5.16	8.99×10^3	3.30×10^3
19068+0544			7.84	5.57	3.94	2.02	8	8	8	2	661	0.85		−8.90	−5.28	1.00×10^4	3.69×10^3
19175−0807	V1420 Aql		7.22	4.71	2.66	–0.15	10	10	10	5	636	1.10		−8.84	−5.24	9.65×10^3	2.00×10^3
19455+0920		AFGL4253	11.93	9.34	6.68	3.01	7	6	7	2	538	0.99		−8.58	−5.05	8.11×10^3	1.13×10^4
19548+3035		AFGL2477	10.15	8.94	8.46	6.57	4	5	5	2	*no solution*						
20072+3116	V1969 Cyg	AFGL2513	7.54	5.30	3.43	0.95	9	9	9	4	706	0.96		−9.00	−5.36	1.07×10^4	3.07×10^3
20082+3228			11.56	8.68	6.14	2.82	5	6	6	2	654	0.91		−8.88	−5.27	9.93×10^3	1.01×10^4
20171+3519			11.72	10.91	8.04	3.74	3	4	5	2	860	0.94	:	−9.31	−5.58	1.32×10^4	2.94×10^4
20435+3825			11.46	8.45	5.84	2.17	8	9	9	4	487	0.49	:	−8.43	−4.94	7.32×10^3	7.13×10^3
20532+5554	V703 Cep		11.95	8.99	6.26	2.49	5	9	9	2	656	0.94		−8.89	−5.28	9.97×10^3	1.07×10^4
20570+2714	V442 Vul	AFGL2686	9.49	6.83	4.21	0.63	9	8	8	5	659	1.06		−8.90	−5.28	1.00×10^4	4.19×10^3
21003+4801			10.54	7.84	5.35	2.08	6	7	7	4	766	0.55		−9.13	−5.45	1.17×10^4	7.87×10^3
21027+5309	V1899 Cyg	AFGL2699	9.71	7.33	5.15	2.29	8	8	8	5	662	0.69		−8.90	−5.29	1.00×10^4	6.47×10^3
21147+5110			13.18	11.34	8.40	3.86	6	7	8	4	772	0.99		−9.14	−5.46	1.18×10^4	3.21×10^4
21223+5114			13.35	10.05	7.14	3.40	4	5	6	2	663	0.88		−8.91	−5.29	1.01×10^4	1.62×10^4
21373+4540			11.35	8.69	6.21	2.78	5	8	8	3	644	0.87		−8.86	−5.25	9.77×10^3	1.03×10^4
21449+4950	V2358 Cyg		11.43	8.65	6.24	3.13	6	8	8	2	665	0.60	:	−8.91	−5.29	1.01×10^4	1.07×10^4
22241+6005	V384 Cep	AFGL2901	9.60	6.91	4.42	1.19	8	9	9	4	641	0.74	:	−8.85	−5.25	9.73×10^3	4.51×10^3
23174+5941	V571 Cas		9.43	7.16	5.22	2.73	9	9	9	4	509	0.63	:	−8.50	−4.99	7.66×10^3	5.54×10^3
23279+5336			9.86	7.54	5.40	2.85	7	6	8	5	583	0.69	:	−8.71	−5.14	8.81×10^3	6.64×10^3

the number of datapoints in the corresponding filter. A ":" after the *K*-band amplitude indicates uncertainties in period and amplitude determination mostly because of poor sampling of the light curves.

To visualise our attempts to fit the observed light curves, Fig. 1 gives five examples. It is obvious that the phase coverage of our NIR measurements is not comparable with well-sampled light curves in the visual. Sometimes it is better to speak of multi-epoch photometry. Nevertheless it can be used to estimate a better average luminosity or at least to get a lower limit for the pulsational amplitudes in the infrared.

Only a few objects of our sample have already published periods. In total, 13 stars were also independently monitored by Whitelock et al. (2006). For two C stars we came to exactly (within a few days) the same periods, namely, IRAS 18239−0655 and 20570+2714, which is quite a surprise given the intrinsic uncertainties in period determination as discussed above. Seven additional objects only deviate up to about 10% in their periods. Using our new periods the datasets of IRAS 06226−0905, 06487+0551, 17581−1744, 18240+2326, 18397+1738 (see Fig. 1), 18398−0220, and 19175−0807 can typically be fitted with residuals of a half or a third of those with the published periods. Nevertheless, taking into account the very small number of points in the individual light curves, this is not a final proof. For only four stars we arrived at different periods. In the case of IRAS 02152+2822 we found 841 instead of 624 days; for 06088+1909, 405 instead of 493 days; for 06268+0849, 422 instead of 619 days, and for 18040−0941, 605 instead of 519 days. In all cases we tried the published values again but even after wider variations no fit solutions with comparable small residuals could be found. Again, the limited datasets leave some uncertainties since the results could be different with only a few points added or deleted.

A quite similar comparison was carried out for the few objects that have positional counterparts (variables within one arcminute) in the NSVS (see above, for ASAS no counterparts were found). In the case of NSVS six stars match the J2000 IRAS coordinates within only 5 arcsec. Three NSVS objects, corresponding to IRAS 03192+5642, 19029+2017 and 19068+0544 support our period findings very well.

The three others, IRAS 01105+6241, 18040−0941, and 18397+1738, all show very well defined but quite different variability in their NSVS data sets, in the 250 to 650 day period ranges with amplitudes well below 1 mag. All are clearly

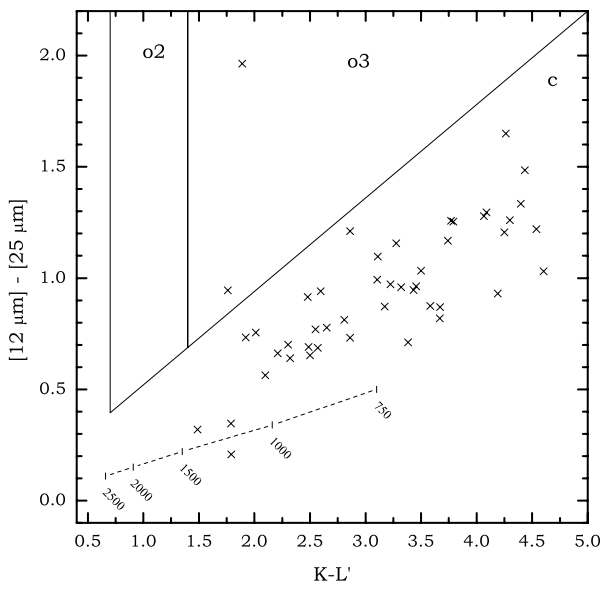

Fig. 2. Infrared two colour diagram according to that of Epchtein et al. (1987) to discriminate O-rich from carbon stars. The colours for blackbodies of different temperatures [K] are indicated. The two outliers in box "o3" are discussed in the text.

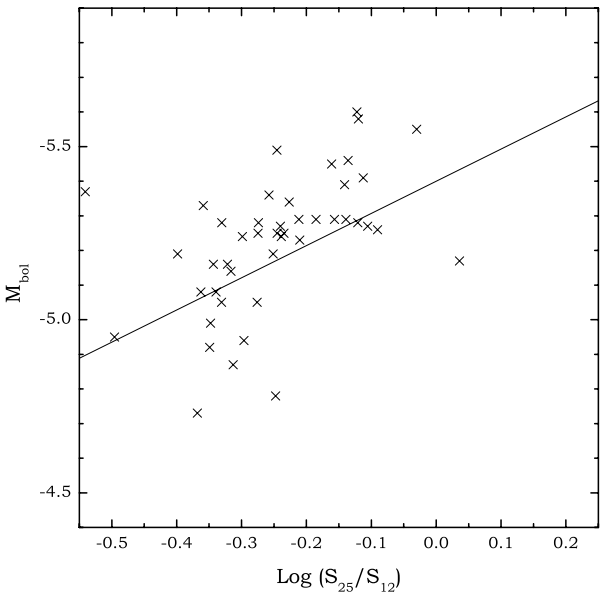

Fig. 3. Bolometric magnitude and IRAS flux-ratio. The line indicates the relation given in Groenewegen et al. (2002).

incompatible with our IR material. The most probable interpretation is in terms of an incidental positional association.

3.2. Mean colours

Using the light curve fits described above, it is possible to derive mean magnitudes in all filters. For some objects with very few measurements in certain colours (mainly $L'_{\rm m}$), no fit was possible and the mean colour index between simultaneous measurements in K and the respective other filter "X" was used to calculate the colour index between the mean K magnitude $K_{\rm m}$ and "$X_{\rm m}$".

Taking our mean colour indices and corresponding IRAS fluxes[1] from the IRAS point source catalogue (PSC, 1988), the infrared two colour diagram shown in Fig. 2 was produced. Following Epchtein et al. (1987), it can be used to characterise AGB objects according to their mass loss rates and chemical properties. Regions "o2" and "o3" contain mainly O-rich stars with increasing mass loss towards higher ($K - L'$) indices. To the left of them, "pure" photosphere without mass loss would be situated. Below in the large area denoted "c", towards the blackbody line, carbon stars of different mass loss rates can be found. Again, higher rates are found to the right.

The aim of the original selection described in Sect. 2 was to select carbon stars. The data points in Fig. 2 confirm the carbon star nature for the overall majority of the stars.

The star located at $(K - L) = 1.76$ and $[12\ \mu\mathrm{m}]-[25\ \mu\mathrm{m}] = 0.95$ is IRAS 03192+5642. It is located quite close to the borderline between regions "o3" and "c". This is unquestionably a carbon star because of its strong SiC feature and its listing in the "General catalog of galactic carbon stars" (Alksnis et al. 2001).

The object located far outside region "c" in the upper part of Fig. 2 is IRAS 19548+3035 (AFGL 2477). This object was previously studied by Groenewegen et al. (1996). This is a very interesting star with a bi-modal spectral energy distribution with a M6S star dominating the light from the optical up to ~3 μm and optically thick carbon-rich material (as evidenced from the IRAS LRS spectrum and molecular line emission) emitting longwards. The *JHK* magnitudes trace the M6S star and our observations then imply that this star is not variable. Our magnitudes are in good agreement with 2MASS (J = 10.20, H = 8.98, K = 8.46). Our new observations do not resolve the nature of this object, which could be a chance coincidence on the sky, or a peculiar binary system with two AGB stars possibly in a disk configuration (Groenewegen et al. 1996).

3.3. Absolute magnitudes and distances

Using the period-luminosity and period-K magnitude relations given in Groenewegen & Whitelock (1996), absolute K magnitudes $M_{\rm K}$, bolometric magnitudes $M_{\rm bol}$, as well as luminosities L were calculated and listed in Table 1. Together with the mean apparent K magnitudes individual distances $r_{\rm K}$ could be derived and are also listed there.

In Groenewegen et al. (2002), a relation between bolometric magnitudes and an IRAS flux ratio was established to derive distances. Our independent dataset can be used to check this relation. The corresponding plot is shown in Fig. 3. For reasons discussed above, IRAS 19548+3035 was omitted in the figure.

4. Discussion and conclusions

Near-infrared observations for a sample of 47 infrared carbon stars are presented, with reliable periods for 31 of them. All amplitudes are such that these objects are Mira type variables. The longest two periods are 840 and 870 days, only slightly longer than the previously longest known period for a galactic carbon star of 783 days. Still, this is considerably shorter than the periods of some OH/IR stars. As the present survey was targeted at carbon stars that are likely to be among those with the longest periods expected, this difference appears real.

[1] The use of IRAS-PSC magnitudes varies in the literature. Both zero point corrected and not zero point corrected values are found. To avoid confusion, for this paper we defined a zero point corrected $[x\,\mu\mathrm{m}] \equiv -2.5 \cdot \log(F/F_0)_{x\mu\mathrm{m}}$. The F_0-values were taken from the IRAS-PSC.

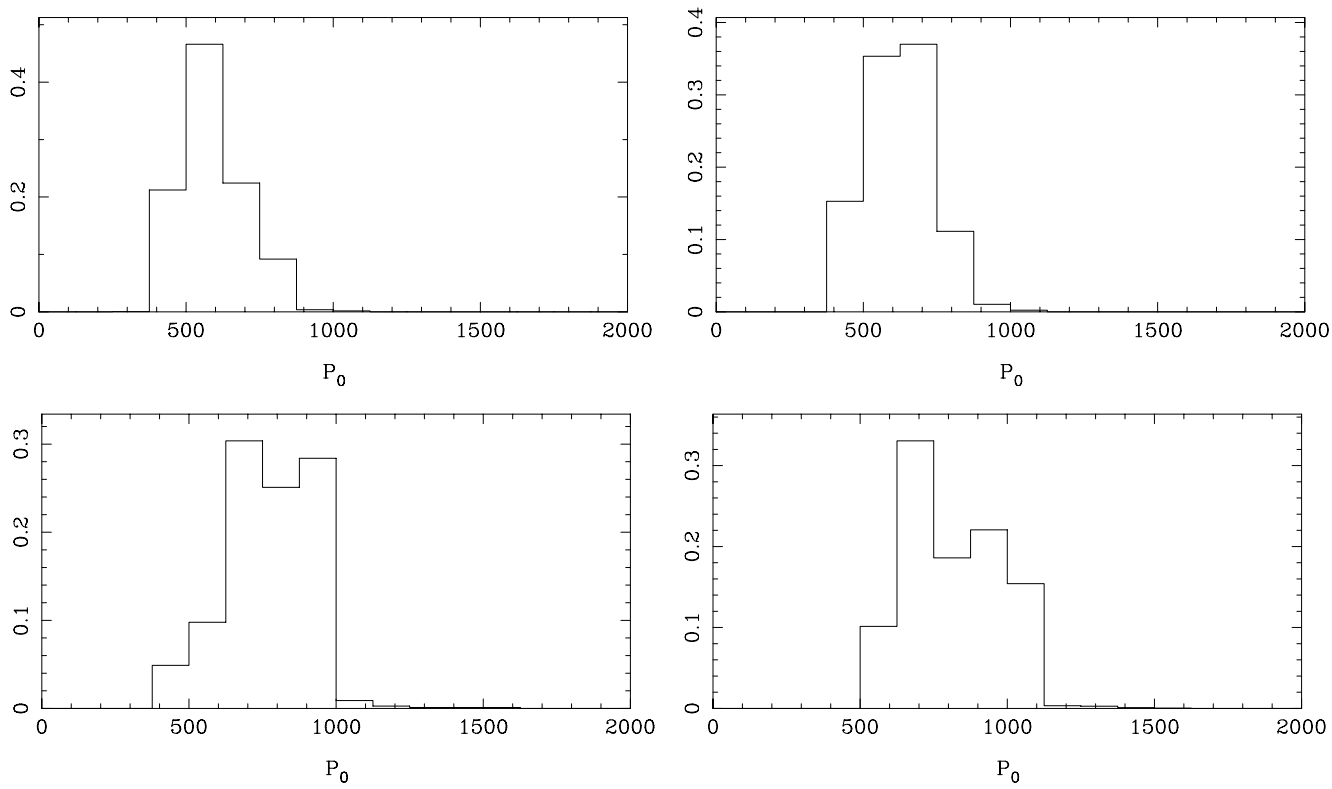

Fig. 4. Theoretical period distribution of AGB stars inside the observed instability strip for carbon stars for masses of 2.5, 2.6, 3.0 (all at $Z = 0.016$), and 3.0 (at $Z = 0.010$) $M_\odot$ (*left to right*, *top to bottom*). Every histogram is normalised to unity.

To try to quantify the relation between pulsation period and stellar evolution, synthetic AGB evolutionary models have been calculated, very similar to the ones described in detail in Appendix C of Groenewegen & Blommaert (2005).

In brief, the synthetic AGB code of Wagenhuber & Groenewegen (1998) was fine-tuned to reproduce the models of Vassiliadis & Wood (1993; hereafter VW) and then extended to more initial masses, including mass loss on the RGB. For several initial masses the fundamental mode period distribution was calculated for stars inside observed instability strips. Contrary to the calculations presented in Groenewegen & Blommaert (2005) where only the optically visible phase was considered, the present work considers the entire LPV phase.

In the present work two *PL* relations are considered, that of Feast et al. (1989) for O-rich stars,

$$M_{\rm bol} = -3.00\ \log P + 2.85, \quad (1)$$

and that of Groenewegen & Whitelock (1996) for C stars,

$$M_{\rm bol} = -2.59\ \log P + 2.02. \quad (2)$$

For each timestep in the synthetic AGB calculation the fundamental period is calculated following VW. The star is assumed to be in the Mira instability strip when the bolometric magnitude is within 0.20 magnitude (the assumed width of the instability strip at a given period) of the *PL* relation.

Table 2 lists the AGB lifetime (defined as the time between the first model in the file (the start of the AGB) up to the point where the remaining envelope mass becomes less than 0.04 $M_\odot$, or $T_{\rm eff} > 4500$ K, that is taken as the start of the post-AGB evolution) for several initial masses, and the LPV lifetime for both *PL* relations considered.

Figures 4 and 5 display the distribution of the fundamental period considering the *PL* relation for C- and O-rich stars, respectively. For the O-rich stars, periods of $\gtrsim$1500 days are reached for the most massive star considered, in agreement with observations. The calculations predict that for a 2.5 $M_\odot$ the fraction of time spent in the C star *PL* relation at periods of $\gtrsim$900 days is only 0.1%, for 2.6 $M_\odot$ stars this is 1%, while for 3.0 $M_\odot$ stars it is already ∼30%. A model for a 3 $M_\odot$ star at a lower metallicity is presented and this object spends more time at the longest periods. These calculations qualitatively reproduce the observations that the longest known period is slightly longer in the LMC than in the Galaxy. The calculations also suggest that the upper mass limit for C star formation is near 2.6 $M_\odot$.

This "critical" initial mass limit does depend on the adopted mass loss rate. The last two entries of Table 2 are for a Reimers

Table 2. AGB and LPV lifetimes.

Z	Mass	AGB lifetime	LPV lifetime	
			O	C
	($M_\odot$)	(10^3 years)	(10^3 years)	(10^3 years)
0.016	2.5	2269	101	49
0.016	2.6	2301	70	43
0.016	3.0	1643	36	35
0.016	3.5	497	25	26
0.016	4.0	232	18	21
0.016	4.5	191	16	19
0.016	5.0	175	15	14
0.010	2.5	2088	78	45
0.010	2.6	2092	59	45
0.010	3.0	1434	32	33
0.016	2.8	2141[1]	207[1]	257[1]
0.016	3.1	894[2]	107[2]	133[2]

[1] For a Reimers mass loss with scaling factor 1.7. [2] For a Reimers mass loss with scaling factor 4.0.

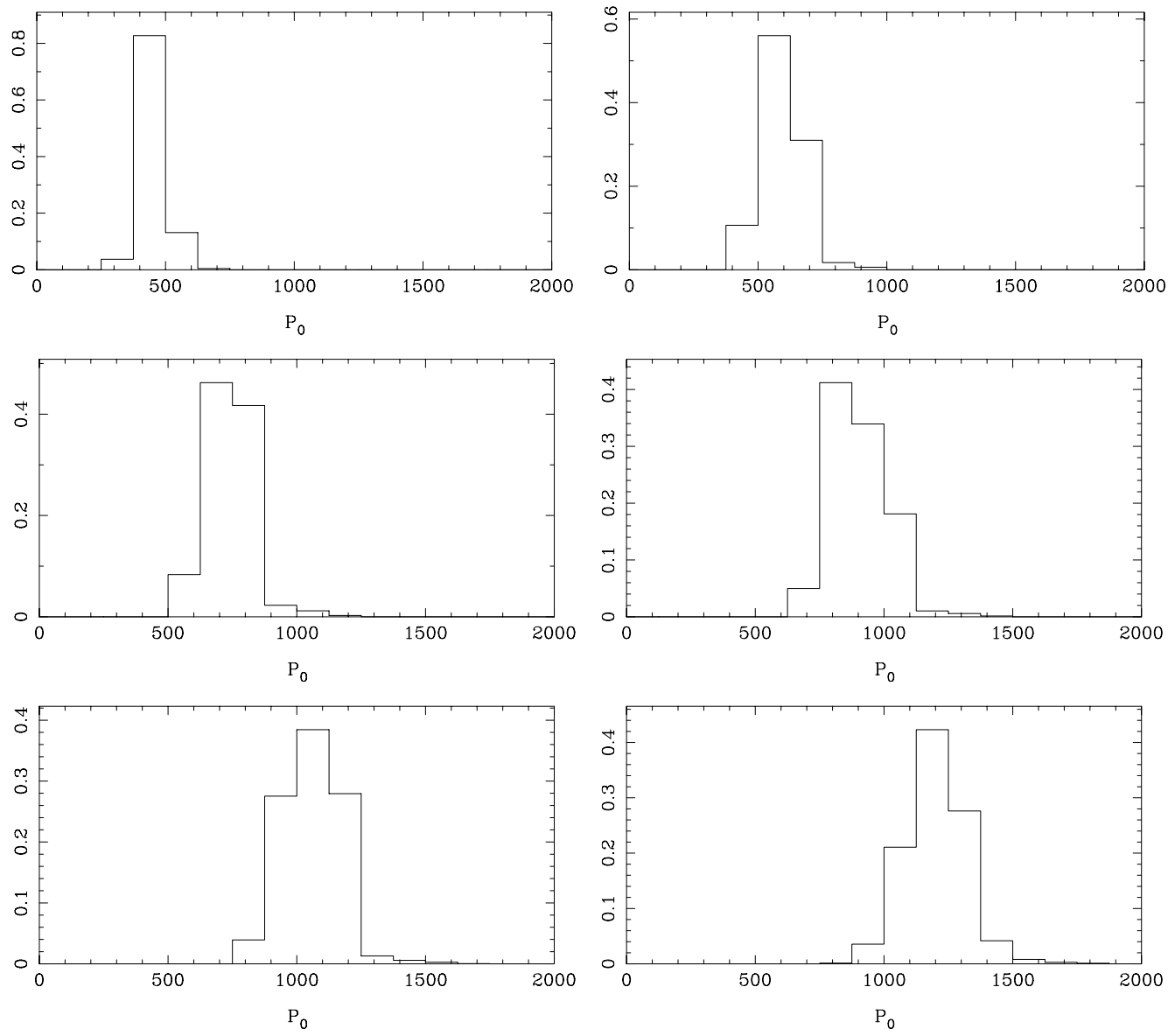

Fig. 5. Theoretical period distribution of AGB stars inside the observed instability strip for oxygen-rich stars for masses of 2.5, 3.0, 3.5, 4.0, 4.5, and 5.0 $M_{\odot}$ (*left to right*, *top to bottom*). Every histogram is normalised to unity.

mass loss rate. One for a scaling factor of 1.7, which was fine-tuned to give the same AGB lifetime as the VW model for a 2.5 $M_{\odot}$ star. In that case the initial mass that gives a 1% probability of having a period of ≳900 days inside the C star stability strip is raised to 2.8 $M_{\odot}$. The last model is for a Reimers scaling factor of 4.0, which is the preferred value from Groenewegen et al. (1995), based on several considerations. In that case the "critical" initial mass is 3.1 $M_{\odot}$.

The main argument for an upper limit in initial mass for C star formation is the process of Hot Bottom Burning (HBB) where carbon is converted to nitrogen. The main confirmation of this is the fact that almost all of the brightest AGB stars in the LMC are oxygen-rich and lithium-rich (e.g., Smith et al. 1995). As an aside it is noted that at the very end of the AGB the envelope mass drops so low that HBB stops, and the star may again become a C star if a third dredge-up occurs again. This implies that in a rare case a carbon star may appear as a Mira variable, probably at a period much longer than 900 days.

Theoretical predictions by Mazzitelli et al. (1999) and Ventura et al. (2000) indicate that HBB occurs for initial masses ≳4 $M_{\odot}$, but this depends on the level of core overshoot and convective mixing, and mass loss. This mass limit is higher than that derived from the longest period of carbon stars. It is unclear how to resolve this discrepancy. Probably only dedicated stellar evolutionary calculations including dredge-up and considering various mass loss rates and input physics can show if the longest period for C stars can be linked directly to the onset of HBB, and at which initial mass.

Acknowledgements. The work of F.K. was supported by APART (Austrian Programme for Advanced Research and Technology) from the Austrian Academy of Sciences.

References

Alksnis, A., Balklavs, A., Dzervitis, U., et al. 2001, BaltA, 10, 1
Elitzur, M., & Ivezić, Ž. 2001, MNRAS, 327, 403
Epchtein, N., Le Bertre, T., Lepine, J. R. D., et al. 1987, A&AS, 71, 39
Feast, M. W., Glass, I. S., Whitelock, P. A., & Catchpole, R. M. 1989, MNRAS, 241, 375
Fraser, O. J., Hawley, S. L., Cook, K. H., & Keller, S. C. 2005, AJ, 129, 768
Groenewegen, M. A. T. 2004, A&A, 425, 595

Groenewegen, M. A. T., & Blommaert, J. A. D. L. 2005, A&A, 443, 143
Groenewegen, M. A. T., & Whitelock, P. 1996, MNRAS, 281, 1347
Groenewegen, M. A. T., Oudmaijer, R. D., Goudfrooij, P., van den Hoek, L. B., & van Kerkwijk, M. H. 1996, A&A, 305, 475
Groenewegen, M. A. T., Van den Hoek, L. B., & de Jong, T. 1995, A&A, 293, 381
Groenewegen, M. A. T., Sevenster, M., Spoon, H. W. W., & Pèrez, I. 2002, A&A, 390, 501
Höfner, S. 1999, A&A, 346, L9
Höfner, S., Jørgensen, U. G., Loidl, R., & Aringer, B. 1998, A&A, 340, 497
IRAS Science Team 1988, IRAS Catalogs and Atlases, Volumes 2–6, NASA RP–1190
Ita, Y., Tanabé, T., Matsunaga, N., et al. 2004, MNRAS, 347, 720
Jones, T. J., Bryja, C. O., Gehrz, T. E. H., et al. 1990, ApJS, 74, 785
Kastner, J. H., Forveille, T., Zuckerman, B., & Omont, A. 1993, A&A, 275, 163
Kiss, L., & Bedding, T. 2004, MNRAS, 347, L83
Koornneef, J. 1983a, A&AS, 51, 489
Koornneef, J. 1983b, A&A, 128, 84
Le Bertre, T. 1992, A&AS, 94, 377
Lebzelter, T. 1999, A&A, 351, 644
Loumos, G. L., & Deeming, T. J. 1978, Ap&SS, 56, 285
Loup, C., Forveille, T., Omont, A., & Paul, J. F. 1993, A&AS, 99, 291
Mazzitelli, I., D'Antona, F., & Ventura, P. 1999, A&A, 348, 846
Nowotny, W., Lebzelter, T., Hron, J., & Höfner, S. 2005, A&A, 437, 285
Pojmansky, G. 2002, Acta Astronomica, 52, 397
Rejkuba M. 2004, A&A, 413, 903
Smith, V. V., Plez, B., Lambert, D. L., & Lubowich, D. A. 1995, ApJ, 441, 735
Sperl, M. 1998, Comm. Asteroseismology (Vienna), 111, 1
van Langevelde, H. J., van der Heiden, R., & van Schooneveld, C. 1990, A&A, 239, 193
Vassiliadis, E, & Wood, P. R. 1993, ApJ, 413, 641 (VW)
Ventura, P., Mazzitelli, I., & D'Antona, F. 2000, A&A, 363, 605
Wagenhuber, J., & Groenewegen, M. A. T. 1998, A&A, 340, 183
Whitelock, P. A., Feast, M. W., van Loon, J. Th., & Zijlstra, A. A. 2003, MNRAS, 342, 86
Whitelock, P. A., Feast, M. W., Marang, F., & Groenewegen, M. A. T. 2006, MNRAS, 369, 751
Winters, J. M., Keady, J. J., Gauger, A., & Sada, P. V. 2000, A&A, 359, 651
Wood, P. R., Alcock, C., Allsman, R. A., et al. 1999, in Asymptotic Giant Branch Stars, ed. T. Le Bertre, A. Lèbre, & C. Waelkens, IAU Symp., 191, ASP, 151
Wozniak, P. R., Vestrand, W. T., Akerlof, C. W., et al. 2004, AJ, 127, 2436

Online Material

Table A.1. Mean total errors of NIR photometry.

Mag	σ_J	σ_H	σ_K	$\sigma_{L'}$
<5	$0\overset{m}{.}02$	$0\overset{m}{.}02$	$0\overset{m}{.}02$	$0\overset{m}{.}02$
5–8	$0\overset{m}{.}03$	$0\overset{m}{.}02$	$0\overset{m}{.}02$	$0\overset{m}{.}04$
8–11	$0\overset{m}{.}04$	$0\overset{m}{.}03$	$0\overset{m}{.}03$	
11–14	$0\overset{m}{.}06$			

Appendix A: NIR photometry

Estimates of the mean total errors of the NIR photometry are given in Table A.1. The given values are calculated from the individual programme- and standard-star measurements. The errors do not include uncertainties of the photometric system.

Table A.2 lists all near-infrared photometry presented in this paper. Besides IRAS name, the modified Julian day number is given.

Table A.2. Individual NIR photometry.

IRAS	MJD	*J*	*H*	*K*	*L′*
01105+6241	50407.0	4.97	3.24	1.90	0.27
01105+6241	50498.0	4.34	2.69	1.42	
01105+6241	50644.0	4.58	2.86	1.54	−0.11
01105+6241	50690.0	4.91	3.16	1.78	
01105+6241	50707.0	5.06	3.30	1.91	0.23
01105+6241	51085.1	5.15	3.78	2.77	0.56
01105+6241	51144.9	4.13	2.58	1.34	
02152+2822	50303.0		9.40	6.31	
02152+2822	50303.0		9.35	6.30	
02152+2822	50407.0	12.11	9.31	6.31	2.05
02152+2822	50692.0	13.30	10.93	7.81	
02152+2822	50708.0	13.30	10.94	7.83	3.22
02152+2822	50809.0	13.10	10.76	7.65	
02152+2822	51086.1	12.80	9.54	6.52	
03192+5642	50303.0	9.31	7.01	5.27	
03192+5642	50303.0	9.19	6.93	5.21	
03192+5642	50408.0	8.06	6.01	4.50	2.51
03192+5642	50690.0	9.19	6.90	5.18	
03192+5642	50692.0	9.13	6.85	5.14	
03192+5642	50707.0	8.98	6.74	5.08	3.23
03192+5642	51085.2	9.59	7.33	5.37	3.93
03192+5642	51144.9	8.68	6.47	4.85	
03238+6034	50303.0		9.32	6.82	
03238+6034	50303.0		9.20	6.82	
03238+6034	50408.0	11.90	8.84	6.47	3.16
03238+6034	50498.0		7.81	5.56	
03238+6034	50692.0	10.86	7.96	5.61	
03238+6034	50709.0	11.20	8.12	5.74	2.57
03238+6034	50809.0	12.20	9.34	6.73	
03238+6034	50877.0	12.40	9.35	6.77	3.30
03238+6034	51085.2	11.40	8.77	6.41	3.67
03238+6034	51144.9	10.20	7.51	5.21	
03385+5927	50303.0		8.90	6.32	
03385+5927	50303.0		8.76	6.20	
03385+5927	50408.0	11.26	8.34	5.81	2.42
03385+5927	50498.0		9.14	6.51	
03385+5927	50690.0		10.57	7.79	
03385+5927	50692.0	12.80	10.64	7.83	
03385+5927	50811.0	12.60	10.67	7.73	
03385+5927	50877.0	12.90	9.44	6.70	
03385+5927	51087.1	11.60	8.73	6.09	2.48
03385+5927	51145.0	12.10	9.43	6.68	
03448+4432	49970.0	14.90	11.49	8.20	3.80
03448+4432	50303.0		9.60	6.56	
03448+4432	50407.0	12.66	9.70	6.72	2.58
03448+4432	50690.0		11.42	7.87	
03448+4432	50692.0	14.30	11.17	7.91	
03448+4432	50708.0	15.90	11.14	7.91	3.70
03448+4432	50809.0	13.50	10.96	7.57	
03448+4432	51145.0	12.40	9.74	6.68	
04179+5951	50303.0		8.20	5.94	
04179+5951	50303.0		8.26	6.00	
04179+5951	50498.0		8.30	6.04	
04179+5951	50691.0	10.04	7.45	4.93	
04179+5951	50809.0	11.15	8.39	5.94	
04179+5951	51085.2		8.06	6.06	3.20
04179+5951	51145.0	9.52	7.01	4.85	
05136+4712	50303.0		9.75	7.23	
05136+4712	50407.0	10.85	8.40	6.22	2.92
05136+4712	50497.0		8.33	6.11	

Table A.2. continued.

IRAS	MJD	J	H	K	L'
05136+4712	50690.0		9.80	7.45	
05136+4712	50692.0	12.30	9.77	7.47	
05136+4712	50709.0	12.70	9.86	7.55	4.08
05136+4712	50877.0	11.70	9.34	7.05	3.60
05136+4712	51087.2	10.80	8.21	6.00	2.69
05136+4712	51147.1	11.50	8.99	6.74	
06088+1909	50407.0	8.81	6.60	4.72	2.40
06088+1909	50498.0	9.26	7.04	5.19	
06088+1909	50690.0	7.65	5.60	3.84	
06088+1909	50809.0	8.92	6.70	4.89	
06088+1909	50811.0	8.92	6.73	4.96	
06088+1909	50877.0	9.00	6.79	4.89	
06088+1909	51145.1	7.72	5.66	3.94	
06226−0905	50407.0	3.96	2.55	1.45	0.04
06226−0905	50690.0	5.25	3.52	2.09	
06226−0905	50707.0	5.15	3.44	2.07	0.51
06226−0905	50908.0	4.44	2.84	1.58	0.09
06226−0905	51145.1	5.76	4.00	2.51	
06268+0849	50407.0	8.41	6.30	4.49	1.94
06268+0849	50690.0	8.85	6.67	4.74	
06268+0849	50709.0	8.78	6.62	4.72	2.12
06268+0849	50811.0	8.70	6.90	4.80	
06268+0849	50877.0	8.03	5.94	4.17	1.53
06268+0849	51145.1	9.54	7.34	5.26	
06487+0551	50408.0	8.37	6.19	4.30	1.87
06487+0551	50690.0	9.30	6.88	4.74	
06487+0551	50709.0	9.42	7.04	5.03	2.46
06487+0551	50809.0	9.51	7.03	4.99	
06487+0551	51145.1	8.26	6.08	4.21	
06487+0551	51292.8	9.20	6.81	5.02	
06531−0216	50407.0	5.99	4.29	2.90	1.11
06531−0216	50497.0	6.55	4.83	3.31	
06531−0216	50707.0	6.90	5.06	3.52	
06531−0216	50811.0	7.43	5.75	4.32	
06531−0216	51145.1	7.57	5.70	3.99	
06531−0216	51292.9	7.13	5.11	3.67	
17581−1744	50268.0	7.12	5.15	3.42	1.28
17581−1744	50303.0	6.98	4.93	3.32	
17581−1744	50642.0	8.61	6.47	4.61	2.06
17581−1744	50690.0	8.31	6.13	4.32	
17581−1744	50692.0	8.33	6.13	4.32	
17581−1744	50708.0	8.37	6.16	4.36	2.08
17581−1744	50908.0	7.42	5.30	3.58	1.31
17581−1744	50947.0	7.53	5.35	3.63	1.36
17581−1744	51292.2	8.80	6.31	4.37	
17581−1744	51393.0	7.45	5.24	3.53	
18040−0941	50268.0	6.61	3.38	1.75	0.30
18040−0941	50303.0	5.61	3.55	1.91	
18040−0941	50643.0	6.90	4.71	2.92	0.52
18040−0941	50691.0	6.64	4.39	2.59	
18040−0941	50709.0	6.52	4.30	2.56	0.26
18040−0941	50985.0	6.19	3.91	2.18	−0.06
18040−0941	51293.1	6.97	4.60	2.65	
18040−0941	51393.9	5.98	3.72	1.95	
18239−0655	50268.0	11.16			1.92
18239−0655	50303.0		8.31	5.65	
18239−0655	50303.0		8.22	5.55	
18239−0655	50643.0	9.40	6.80	4.30	1.00
18239−0655	50690.0	9.44	6.72	4.18	

Table A.2. continued.

IRAS	MJD	J	H	K	L'
18239−0655	50692.0	9.38	6.71	4.18	
18239−0655	50947.0	10.58	7.96	5.34	1.73
18239−0655	51293.1	9.27	6.45	3.91	
18239−0655	51394.0	10.11	7.26	4.62	
18239−0655	51394.9	10.19	7.26	4.63	
18240+2326	50265.0	11.13	8.34	5.17	0.73
18240+2326	50303.0		8.10	4.96	
18240+2326	50643.0	13.00	10.22	6.88	2.04
18240+2326	50692.0	11.80	10.19	6.83	
18240+2326	50709.0	12.90	9.95	6.70	1.98
18240+2326	50947.0	11.14	8.38	5.23	0.74
18240+2326	51086.9	11.60	8.93	5.65	1.12
18240+2326	51292.1	12.10	10.50	7.04	
18244−0815	50268.0	10.32			2.39
18244−0815	50303.0		7.42	5.12	
18244−0815	50643.0		9.61	6.44	3.13
18244−0815	50691.0		8.96	6.35	
18244−0815	50709.0	10.55	8.93	6.36	3.20
18244−0815	50908.0	11.00	7.83	5.30	2.37
18244−0815	50947.0	10.79	7.94	5.47	2.45
18244−0815	51292.2	12.50	9.40	6.39	
18248−0839	50268.0	12.60			2.50
18248−0839	50303.0			6.95	
18248−0839	50303.0			6.95	
18248−0839	50643.0	11.70	8.60	5.60	1.60
18248−0839	50690.0		8.45	5.37	
18248−0839	50692.0	12.02	8.43	5.37	
18248−0839	50709.0	11.95	8.40	5.34	1.44
18248−0839	50947.0	13.20	10.13	6.91	2.54
18248−0839	51293.1	11.60	8.75	5.64	
18269−1257	50303.0			7.95	
18269−1257	50644.0		9.42	5.73	1.94
18269−1257	50692.0	15.40	8.99	5.81	
18269−1257	50947.0	12.40	10.30	9.28	
18269−1257	51293.2		9.64	6.24	
18269−1257	51394.9		9.52	5.80	
18320−0352	50303.0			7.54	
18320−0352	50644.0		12.00	9.10	4.70
18320−0352	50691.0			8.98	
18320−0352	50985.0	13.80	10.71	7.56	3.18
18320−0352	51086.8	13.20	11.06	7.96	3.95
18320−0352	51294.1	12.00	11.30	8.75	
18367−0452	50303.0			8.82	
18367−0452	50644.0	12.40	10.23	7.34	2.77
18367−0452	50690.0		10.49	7.59	
18367−0452	50692.0	12.45	10.47	7.59	
18367−0452	50948.0	11.69	10.67	8.83	4.25
18367−0452	50985.0	12.50	10.94	8.77	4.05
18367−0452	51086.8	12.10	10.65	7.72	4.00
18367−0452	51294.1	11.60	9.88	7.30	
18397+1738	50265.0	4.72	2.83	1.17	−1.23
18397+1738	50303.0	4.60	2.78	1.15	
18397+1738	50303.0	4.52	2.70	1.05	
18397+1738	50643.0	5.62	3.80	2.08	−0.49
18397+1738	50692.0	5.05	3.18	1.44	
18397+1738	50708.0	4.93	3.06	1.34	−1.10
18397+1738	50908.0	5.85	3.79	1.93	−0.67
18397+1738	50947.0	6.18	4.12	2.23	−0.43
18397+1738	50986.0	6.48	4.40	2.53	−0.21
18397+1738	51086.9	6.42	4.29	2.31	−0.27

Table A.2. continued.

IRAS	MJD	J	H	K	L'
18397+1738	51292.1	5.01	2.95	1.19	
18398−0220	50303.0	4.98	2.94	1.31	
18398−0220	50303.0	4.98	3.00	1.41	
18398−0220	50643.0	5.79	3.76	2.08	−0.12
18398−0220	50691.0	5.53	3.46	1.83	
18398−0220	50947.0	4.81	2.83	1.25	−0.97
18398−0220	51085.8	5.88	3.66	1.83	
18398−0220	51294.2	6.26	4.05	2.21	
18424+0346	50303.0	8.36	5.84	3.82	
18424+0346	50303.0	8.38	5.72	3.73	
18424+0346	50643.0	9.16	6.70	4.58	1.78
18424+0346	50690.0	8.62	6.13	4.03	
18424+0346	50692.0	8.53	6.08	4.02	
18424+0346	50975.0	10.27	7.92	5.77	
18424+0346	51086.9	9.76	7.35	5.23	2.73
18424+0346	51292.2	9.09	6.62	4.85	
18475+0926	50265.0	11.29	8.80	5.89	1.73
18475+0926	50303.0		8.90	6.02	
18475+0926	50303.0		8.82	5.74	
18475+0926	50643.0	11.80	9.79	7.22	2.78
18475+0926	50692.0	12.10	9.80	7.16	
18475+0926	50948.0	11.08	8.29	5.59	1.48
18475+0926	50975.0	10.80	8.35	5.61	
18475+0926	50985.0	11.10	8.32	5.58	1.53
18475+0926	51085.9	11.39	8.78	6.05	
18475+0926	51294.1	12.10	10.10	7.23	
19029+0808	50265.0	11.38	8.46	5.44	1.53
19029+0808	50303.0		8.72	5.54	
19029+0808	50643.0	12.00	9.81	7.00	2.45
19029+0808	50691.0		9.41	6.23	
19029+0808	50948.0	10.94	8.03	5.05	1.16
19029+0808	50975.0		8.52	5.22	
19029+0808	50985.0	11.70	8.40	5.26	1.35
19029+0808	51085.9	12.02	9.20	5.99	
19029+0808	51294.2	10.06	8.89	7.18	
19029+0808	51393.0	12.00	9.89	6.81	
19029+2017	50643.0	7.54	5.41	3.64	2.45
19029+2017	50690.0	7.21	5.06	3.33	
19029+2017	50692.0	7.15	5.03	3.30	
19029+2017	50908.0	8.02	5.77	3.90	1.45
19029+2017	50985.0	8.59	6.28	4.35	1.95
19029+2017	51294.1	7.15	5.04	3.30	
19068+0544	50303.0	7.67	5.38	3.62	
19068+0544	50303.0	7.80	5.54	3.80	
19068+0544	50692.0	8.02	5.74	4.04	
19068+0544	50948.0	7.19	4.92	3.46	1.54
19068+0544	50985.0	7.59	5.30	3.68	1.76
19068+0544	51085.9	8.67	6.24	4.39	
19068+0544	51294.2	8.03	5.87	4.34	
19068+0544	51395.0	6.76	4.63	3.20	
19175−0807	50265.0	7.96	5.39	3.14	0.17
19175−0807	50303.0	7.21	4.72	2.97	
19175−0807	50643.0	7.91	5.28	3.05	0.13
19175−0807	50691.0	8.30	5.62	3.34	
19175−0807	50707.0	8.27	5.61	3.36	0.51
19175−0807	50948.0	7.20	4.72	2.67	−0.08
19175−0807	50975.0	6.80	4.33	2.29	
19175−0807	50985.0	6.56	4.05	2.06	−0.50
19175−0807	51085.8	5.86	3.52	1.64	
19175−0807	51294.2	6.72	4.45	2.73	

Table A.2. continued.

IRAS	MJD	J	H	K	L'
19455+0920	50268.0	12.64			3.74
19455+0920	50303.0			7.49	
19455+0920	50642.0	11.97	9.75	6.70	3.03
19455+0920	50692.0	12.47	9.68	7.07	
19455+0920	51085.9	11.10	8.35	5.81	
19455+0920	51146.8	11.80	8.72	6.11	
19455+0920	51293.2	12.20	10.15	7.67	
19455+0920	51394.0	12.60	9.95	7.30	
19548+3035	50268.0	10.28			4.96
19548+3035	50303.0		8.90	8.44	
19548+3035	50303.0		8.88	8.38	
19548+3035	50644.0	10.16	8.95	8.49	6.60
19548+3035	50691.0	10.13	8.92	8.53	
19548+3035	51393.0	10.25	9.03	8.44	
20072+3116	49967.0	7.22	4.92	3.19	0.86
20072+3116	50690.0	6.81	4.61	2.82	
20072+3116	50692.0	6.78	4.61	2.83	
20072+3116	50709.0	6.76	4.56	2.78	0.31
20072+3116	50908.0	6.98	4.74	2.93	0.37
20072+3116	50985.0	7.57	5.28	3.41	0.85
20072+3116	51145.8	8.70	6.33	4.35	
20072+3116	51293.2	8.24	6.10	3.87	
20072+3116	51394.1	7.07	4.85	3.00	
20082+3228	50303.0		7.51	5.19	
20082+3228	50644.0	11.80	9.15	6.58	3.11
20082+3228	50692.0	12.10	9.24	6.61	
20082+3228	50985.0	11.27	8.12	5.62	2.45
20082+3228	51146.8	12.10	9.54	6.91	
20082+3228	51395.0	11.78	8.80	6.20	
20171+3519	50303.0			8.76	
20171+3519	50643.0		10.20	7.00	3.00
20171+3519	50985.0	12.90	13.00	9.00	4.40
20171+3519	51145.9	10.50	9.04	8.47	
20171+3519	51293.2	13.20	11.80	8.09	
20435+3825	50265.0	11.21	8.28	5.88	1.96
20435+3825	50303.0		8.39	5.67	
20435+3825	50642.0	12.03	9.00	6.25	2.64
20435+3825	50692.0	11.36	8.45	5.78	
20435+3825	50707.0	12.01	8.91	6.24	2.73
20435+3825	50986.0	11.90	8.91	6.11	2.48
20435+3825	51145.9	11.70	8.90	6.30	
20435+3825	51293.3	11.70	8.09	5.55	
20435+3825	51395.1	10.25	7.48	5.07	
20532+5554	50303.0		8.55	5.87	
20532+5554	50303.0		8.63	5.93	
20532+5554	50303.0		8.76	6.12	
20532+5554	50642.0	11.82	9.20	6.37	2.60
20532+5554	50691.0		8.63	5.93	
20532+5554	50809.0	11.20	8.19	5.35	
20532+5554	50986.0	12.20	9.21	6.34	2.57
20532+5554	51146.9	13.00	9.96	7.17	
20532+5554	51294.2	12.00	9.10	6.56	
20570+2714	49968.0	9.68	7.01	4.56	0.98
20570+2714	50266.0	9.92			0.92
20570+2714	50303.0	9.07	6.38	3.90	
20570+2714	50642.0	9.96	7.17	4.55	0.99
20570+2714	50692.0	10.30	7.70	5.01	
20570+2714	50709.0	10.51	7.83	5.14	1.35
20570+2714	50986.0	9.15	6.38	3.61	0.21

Table A.2. continued.

IRAS	MJD	J	H	K	L'
20570+2714	51146.9	8.52	5.83	3.32	
20570+2714	51394.1	10.40	7.99	5.28	
21003+4801	50303.0		8.59	6.11	
21003+4801	50643.0	9.86	7.14	4.67	1.46
21003+4801	50644.0	9.93	7.19	4.72	1.42
21003+4801	50692.0	10.10	7.36	4.90	
21003+4801	50708.0	10.22	7.48	5.01	1.75
21003+4801	50986.0	10.61	8.21	5.64	2.31
21003+4801	51145.9	11.00	8.20	5.69	
21027+5309	49972.0	8.96	6.54	4.48	1.81
21027+5309	50268.0	10.20			2.42
21027+5309	50303.0		8.00	5.76	
21027+5309	50408.0	9.74	7.35	5.24	
21027+5309	50643.0	9.02	6.64	4.47	1.67
21027+5309	50691.0	9.33	6.93	4.82	
21027+5309	50707.0	9.56	7.12	4.95	2.07
21027+5309	50986.0	10.50	8.08	5.67	2.58
21027+5309	51146.9	9.22	6.98	4.82	
21147+5110	50268.0	11.93			4.13
21147+5110	50303.0			9.25	
21147+5110	50408.0		11.23	9.42	
21147+5110	50643.0	13.70	11.29	7.91	3.31
21147+5110	50690.0		10.65	7.57	
21147+5110	50691.0	13.04	10.74	7.54	
21147+5110	50708.0	12.80	10.70	7.49	3.13
21147+5110	50986.0	12.70	11.49	8.64	3.99
21147+5110	51147.0	12.50	12.36	9.26	
21223+5114	50303.0			8.13	
21223+5114	50644.0	12.70	9.74	6.79	2.93
21223+5114	50692.0	13.30	9.92	6.96	
21223+5114	50986.0		10.55	7.40	3.78
21223+5114	51146.9	11.90	9.10	6.34	
21223+5114	51394.1	14.00	9.68	6.98	
21373+4540	50303.0		9.53	7.02	
21373+4540	50643.0	10.67	7.88	5.46	2.13
21373+4540	50691.0		8.16	5.78	
21373+4540	50707.0	11.14	8.21	5.82	2.43
21373+4540	50986.0		9.62	6.87	3.29
21373+4540	51086.0	11.30	8.93	6.09	
21373+4540	51146.0	10.40	7.83	5.63	
21373+4540	51394.2	11.40	8.53	6.22	
21449+4950	50303.0		9.03	6.62	
21449+4950	50643.0	11.30	8.45	6.06	2.97
21449+4950	50690.0		8.20	5.90	
21449+4950	50692.0	10.97	8.17	5.87	
21449+4950	50809.0	10.83	8.08	5.59	
21449+4950	50986.0	11.85	9.21	6.51	3.38
21449+4950	51147.0	11.80	9.06	6.63	
21449+4950	51395.1	10.53	7.73	5.47	
22241+6005	50265.0	10.27	7.24	4.63	1.15
22241+6005	50303.0		7.68	4.99	
22241+6005	50644.0	9.14	6.47	4.03	0.87
22241+6005	50690.0	8.82	6.14	3.77	
22241+6005	50692.0	8.81	6.15	3.76	
22241+6005	50809.0	9.03	6.31	3.79	
22241+6005	50811.0	8.84	6.54	3.80	
22241+6005	50986.0				1.62
22241+6005	51087.1	10.41	7.54	5.17	2.14
22241+6005	51146.0	9.61	6.89	4.55	

Table A.2. continued.

IRAS	MJD	J	H	K	L'
23174+5941	50265.0	9.25	6.92	4.99	2.45
23174+5941	50303.0	9.13	6.87	4.95	
23174+5941	50407.0	9.01	6.74	4.84	2.42
23174+5941	50644.0	10.25	7.91	5.87	3.35
23174+5941	50691.0	10.20	7.84	5.78	
23174+5941	50707.0	10.10	7.77	5.74	3.27
23174+5941	50809.0	9.01	6.69	4.67	
23174+5941	51147.0	9.72	7.52	5.63	
23174+5941	51395.1	8.15	6.09	4.44	
23279+5336	50268.0	10.40			2.81
23279+5336	50303.0		8.20	6.02	
23279+5336	50303.0		8.44	6.09	
23279+5336	50407.0	10.46	8.03	5.82	2.93
23279+5336	50644.0	9.12	6.71	4.64	3.35
23279+5336	50690.0	9.57		4.98	
23279+5336	50692.0	9.52		5.00	
23279+5336	50707.0	9.72	7.27	5.14	2.39
23279+5336	51085.1	9.09	7.03	5.16	1.89